Green Chemistry

PAPER

View Article Online
View Journal | View Issue

Check for updates

Cite this: *Green Chem.*, 2024, **26**, 11600

A deamination-driven biocatalytic cascade for the synthesis of ribose-1-phosphate†

Jonas Motter, [a] Sarah Westarp, [a,b] Jonas Barsig, [a] Christina Betz, [a] Amin Dagane,[a] Felix Kaspar, [a,d] Lena Neumair, [a] Sebastian Kemper, [c] Peter Neubauer [a] and Anke Kurreck *[a,b]

Received 18th June 2024,
Accepted 7th October 2024

DOI: 10.1039/d4gc02955k

rsc.li/greenchem

Ribose-1-phosphate (**Rib1P**) is a key substrate for the synthesis of difficult-to-access nucleoside analogues by nucleoside phosphorylases. However, its use in preparative synthesis is hampered by low yields and low selectivity during its preparation by conventional methods. Although biocatalysis permits straightforward access to **Rib1P** directly from natural nucleosides, these transformations are tightly thermodynamically controlled and suffer from low yields and non-trivial work-up procedures. To address these challenges, we developed a biocatalytic cascade that allows near-total conversions of natural guanosine into α-anomerically pure **Rib1P**. The key to this route is a guanine deaminase, which removes the accumulated guanine byproduct. Under optimised conditions, this cascade proved readily scalable to the gram scale, delivering isolated yields of up to 79% and a purity of 94% without any chromatography. Our cascade approach reduced the need for toxic reagents and purification steps inherent to previous methods, reducing the environmental burden of the route, as confirmed by CHEM21 Zero Pass and *E*-factor calculations. Thus, our work will broadly strengthen the applicability of nucleoside phosphorylase-mediated chemistry.

Open Access Article. Published on 14 octobre 2024. Downloaded on 25/01/2026 09:27:58.
This article is licensed under a Creative Commons Attribution 3.0 Unported Licence.

Introduction

Pentose-1-phosphates (P1Ps), such as ribose-1-phosphate (**Rib1P**), are central molecules in the nucleoside salvage pathway. As substrates for nucleoside phosphorylases (NPs), they additionally serve as valuable starting points for the enzymatic synthesis of nucleoside analogues,[1–7] one of the most successful class of small-molecule drugs to treat viral infections[8,9] or cancer,[10,11] and which recently attracted interest as precursors of mRNA vaccines[12,13] and antibacterial agents.[14,15] Employing P1Ps for the synthesis of nucleoside analogues is especially advantageous when product yields are low due to thermodynamic constraints[16–19] or when suitable donor nucleosides are not readily available.[20,21]

Despite its potential for the synthesis of important nucleoside analogues, a high-yielding and sustainable synthesis for P1Ps has not yet been developed. Chemical synthesis routes toward **Rib1P** strongly rely on protection/deprotection steps and show only moderate stereoselectivity, which leads to a mixture of α- and β-anomers.[22] Consequently, only low yields are achieved due to the multi-step synthesis routes and the need for additional purification steps.

Enzymatic and chemoenzymatic approaches using NPs have been developed as a viable alternative, allowing direct biocatalytic access to α-anomeric pure **Rib1P**. NPs catalyse the tightly thermodynamically controlled reversible phosphorolytic cleavage of nucleosides to the corresponding nucleobases and P1Ps.[16–18] Previous NP-based routes toward **Rib1P** are mainly based on natural nucleosides[23–27] or the base-modified 7-methylguanosine (**7-Me-Guo**).[28,29] Using uridine as a substrate for **Rib1P** synthesis, isolated yields of only 31% and 25% were obtained using either *E. coli* UP[23] or thermostable pyrimidine NPs[24] (Fig. 1A). The application of **7-Me-Guo** as a substrate offers the advantage of near-irreversible phosphorolysis due to the *in situ* precipitation of the nucleobase and its low nucleophilicity.[28,29]

Whilst total isolated yields of up to 79% (from guanosine, **Guo**) were achieved using the approach, it has the drawback that an upstream chemical step (using toxic and carcinogenic iodomethane) is required to prepare **7-Me-Guo** (Fig. 1B). In addition, **7-Me-Guo** is labile to hydrolysis and has a low shelf life, making it a non-ideal reagent.

[a]*Chair of Bioprocess Engineering, Institute of Biotechnology, Faculty III Process Sciences, Technische Universität Berlin, Ackerstraße 76, 13355 Berlin, Germany. E-mail: anke.wagner@tu-berlin.de*
[b]*BioNukleo GmbH, Ackerstraße 76, 13355 Berlin, Germany*
[c]*Institute for Chemistry, Technische Universität Berlin, Straße des 17. Juni 135, 10623 Berlin, Germany*
[d]*Institute for Biochemistry, Biotechnology and Bioinformatics, Technische Universität Braunschweig, Spielmannstraße 7, 38106 Braunschweig, Germany*
† Electronic supplementary information (ESI) available. See DOI: https://doi.org/10.1039/d4gc02955k

This journal is © The Royal Society of Chemistry 2024

Open Access Article. Published on 14 octobre 2024. Downloaded on 25/01/2026 09:27:58.
This article is licensed under a Creative Commons Attribution 3.0 Unported Licence.

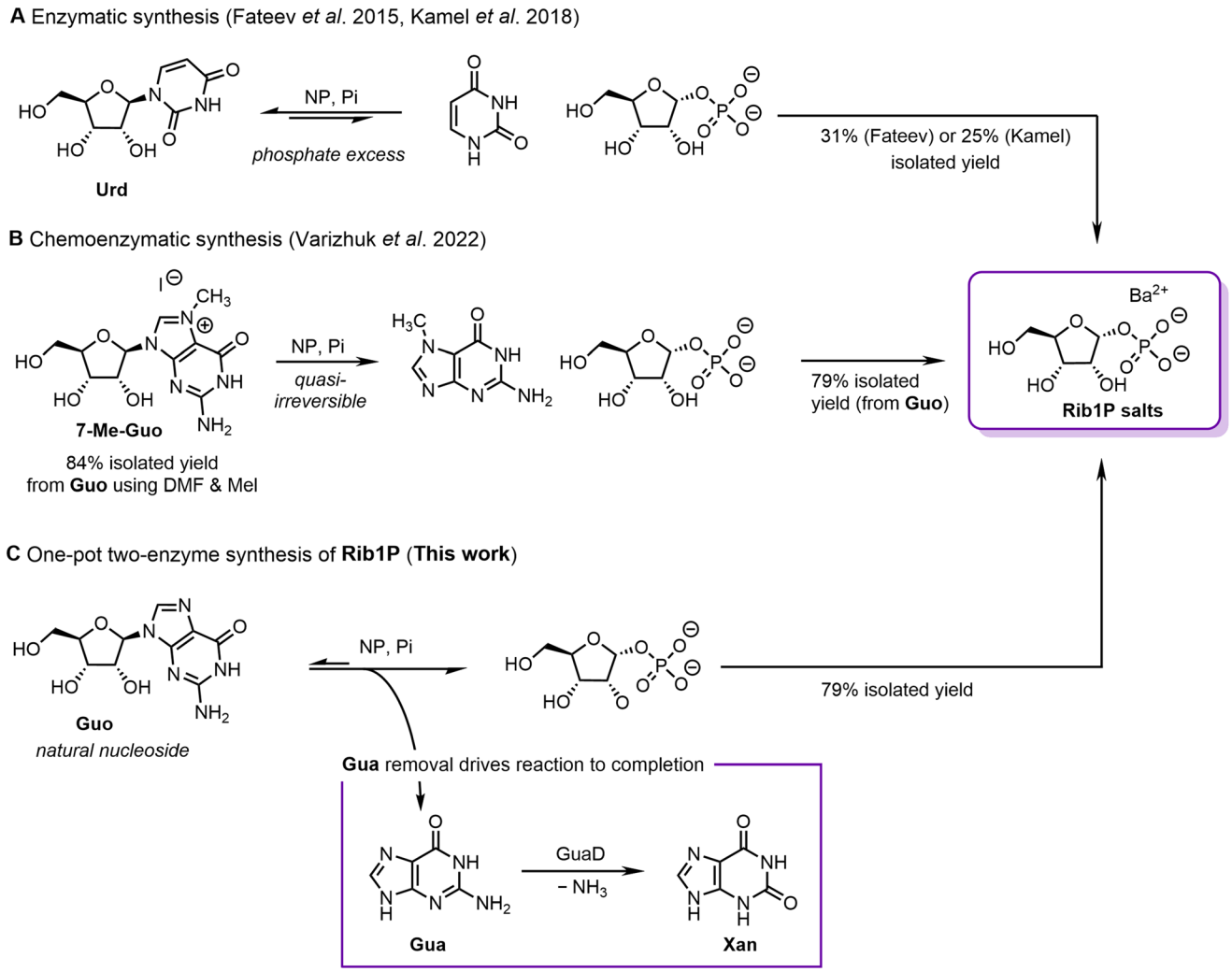

Fig. 1 Strategies for the (chemo)enzymatic synthesis of ribose-1-phosphate (**Rib1P**). (A) Enzymatic synthesis by Fateev *et al.* (2015)[23] and Kamel *et al.* (2018).[24] (B) Chemoenzymatic synthesis by Varizhuk *et al.* (2022).[29] (C) GuaD coupled synthesis as presented in this work. **Urd** = uridine, **Guo** = guanosine, **Gua** = guanine, **Xan** = xanthine.

An *in vitro* biocatalytic cascade involving phosphorolysis and product removal could address these challenges and lead to a high-yielding and sustainable synthesis route of **Rib1P.** Kalckar had already envisioned such a strategy in 1947, by coupling the phosphorolysis of inosine with a xanthine oxidase.[25] Although this approach found a recent application,[27] xanthine oxidases are unstable enzymes and are difficult to produce on scale.[30–35] As such, this vision has not yet been successfully translated into a practical, scalable, high-yielding method that starts from cheap and available substrates and enzymes.

Motivated by these initial efforts, we have developed an enzymatic cascade for the synthesis of **Rib1P** centred around a guanine deaminase (GuaD). Using **Guo** as a substrate for NP-catalysed phosphorolysis permits almost full nucleoside cleavage in the presence of *Deinococcus geothermalis* GuaD (*Dg*GuaD), which converts the accumulating guanine (**Gua**) to xanthine (**Xan**, Fig. 1C). We herein describe how the application of the thermostable *Dg*GuaD in combination with thermostable NPs allowed the development of a scalable synthesis of **Rib1P** from **Guo** in one pot with isolated yields of up to 79%. These processes benefitted from streamlined purification procedures and led to a strongly reduced need for solvents or hazardous chemicals, which was well reflected by improved values of CHEM21 Zero Pass calculations compared to other (chemo)enzymatic approaches. Thus, our work paves the way for a sustainable synthesis of **Rib1P** and its derivatives, further strengthening the feasibility of biocatalytic nucleoside chemistry.

Results and discussion

Development of a two-enzyme cascade for Rib1P synthesis

The ideal biocatalytic cascade for **Rib1P** synthesis uses cheap and commercially available starting materials, achieves full

Open Access Article. Published on 14 octobre 2024. Downloaded on 25/01/2026 09:27:58.
This article is licensed under a Creative Commons Attribution 3.0 Unported Licence.

conversion of an otherwise thermodynamically controlled reaction, requires only a short reaction time and can be integrated smoothly into downstream processing for product isolation. For these reasons, we envisioned that a cascade starting from **Guo** would offer the best combination of these traits when a deaminase converts the liberated nucleobase **Gua** to poorly soluble **Xan**.

Thus, we began our studies searching for a **Gua**-specific, thermostable guanine deaminase (GuaD, EC 3.5.4.3). Thermostability is considered one of the most critical traits for biocatalysts,[36–40] but previously described narrow-spectrum GuaDs lacked significant stability.[41–43] To this end, we screened genomes of well-described thermophilic organisms for guanine deaminases. We selected GuaD of *D. geothermalis* (*Dg*GuaD) as a promising candidate and heterologously expressed the protein in *E. coli*. A preliminary characterisation of the enzyme revealed that *Dg*GuaD showed a narrow substrate spectrum (only **Gua** is accepted), a high specific enzyme activity (1400 U mg^{-1}), and a moderate thermostability (detailed information on enzyme mining and characterisation is provided in Fig. S1–9 and Table S1†).

With the specific and thermostable GuaD in hand, we screened reaction conditions for optimal **Rib1P** synthesis. Since **Guo** is a natural substrate for purine NPs (PNPs, EC 2.4.2.1), we decided to use commercially available PNPs from thermophilic microorganisms. Indeed, in coupled reactions of PNP N04 and *Dg*GuaD in the presence of 0.9 equivalents (eq.) of phosphate, we observed up to 80% **Guo** cleavage. Under the same conditions but without GuaD, only 16% conversion is expected based on thermodynamic calculations (K = 0.04 for **Guo** at 50 °C).[16] Hence, byproduct removal led to a significant increase in **Guo** conversion. **Gua** was immediately converted to **Xan** in our cascade reactions and never accumulated (Fig. 2A).

Despite *Dg*GuaD's high selectivity, this cascade proved to be under kinetic control due to a low degree of promiscuity of PNPs. As such, we observed additional byproducts in addition to **Xan** arising from the glycosylation of **Xan** to give either ***N*9-Xao** or, as recently discovered, ***N*7-Xao**[44] (Fig. 2A and B).

Although the hyperthermophilic PNP N04 proved to be the most **Guo**-selective enzyme among those we screened (at 50 °C), minor amounts of byproduct formation (**Xan** glycosides) were unavoidable (Fig. S10 and 11†). Therefore, we decided to stop the reactions at the maximum **Xan** concentration (the highest conversion point to **Rib1P**). This is crucial as the final reaction equilibrium forms between **Xan** and **Xao**, thereby minimising available **Rib1P** levels (Fig. 2B).

Based on these preliminary results, we optimised the reaction conditions to generate maximum **Rib1P** concentrations. We determined the optimum ratio of the two enzymes under cascade reactions. This involved directly reducing the *Dg*GuaD concentration while maintaining a fixed PNP N04 concentration (with 5 mM **Guo** and 0.9 eq. HPO_4^{2-}) (Fig. 2C). The process was then repeated with the optimum *Dg*GuaD concentration but with varying PNP N04 catalyst loads (Fig. 2D). To further improve **Guo** cleavage, we studied the impact of increasing phosphate excess on the enzymatic cascade. To achieve near-full **Guo** cleavage of >98%, only 1.2 eq. of phosphate was required (Fig. 2E). For comparison, the phosphorolysis of **Guo** would require 1150 eq. of phosphate for 98% conversion (with a K = 0.04 of **Guo** at 50 °C). Since phosphate removal is one of the most critical steps in the production of **Rib1P**,[24] this is a significant improvement over the available enzymatic production methods based on natural substrates. Finally, we determined the maximum **Guo** loading in the reactions. Reactions with **Guo** concentrations >40 mM never completely dissolved (data not shown), and maximum **Guo** conversion significantly decreased (Fig. 2F). Therefore, 25 mM **Guo** was applied for further experiments as all reactants fully dissolved within 15 min (data not shown).

Production of Rib1P at the gram scale

Following optimisation, we aimed to produce **Rib1P** as a barium salt at the gram scale. Therefore, we performed a test run on a 2 mL scale to determine when to terminate the reaction and then upscaled the reaction volume to 150 mL for the production of a first batch of **Rib1P** (Fig. S12A†). After the upscaled reaction was stopped at a conversion of 88%, the enzyme was removed by freezing and thawing the reaction mixture. Taking advantage of the pH-dependent solubility,[45] free **Xan** was precipitated by shifting the pH to ≈7 (Fig. 3A). At this step, approximately 2% of the initial **Xan** remained in the mixture, but ***N*9-Xao** concentration was only slightly affected by the pH shift (as determined by HPLC, Fig. 3B and Fig. S12C†). Further purification was based on our previously published method.[24] Phosphate was precipitated using NH_4Cl and $MgCl_2$. Due to the low phosphate concentration, the need for phosphate-precipitating compounds has been significantly minimised, which reduced the co-precipitation (and therefore loss) of **Rib1P**. Finally, after confirming phosphate precipitation (Fig. S12B†), **Rib1P** was precipitated as its Ba-salt by the addition of ethanol and barium acetate. For the collection of the precipitated **Rib1P**, we compared filtration and centrifugation. Although centrifugation was more prone to residual ethanol contamination, it yielded more **Rib1P** (0.53 g *vs.* 0.45 g after filtration) and was the preferred method due to handling benefits (Fig. S12D†). After repeating the **Rib1P** synthesis and using centrifugation to collect the product, **Rib1P** was obtained with an isolated yield of up to 79% (1.1 g). Product purity was determined by HPLC (Fig. 3B and Fig. S12C†), ^{1}H- and ^{31}P-NMR (Fig. S12D–15†) and by evaluating the performance of **Rib1P** in glycosylation reactions (Fig. 3C). A purity of 94% (obtained for batch 2) was determined by quantitative ^{1}H-NMR (Fig. S12D, see ESI† for NMR data). The main impurities were acetate (3.8%), ethanol (<0.6%) and ***N*9-Xao** (0.5%, also confirmed by HPLC) (Fig. S12C†). Although the pH shift did not strongly impact the ***N*9-Xao** concentration, its precipitation occurred progressively during the purification process due to incubation steps at low temperatures (Fig. 3B), resulting in less than 1% in the final **Rib1P** stock (Fig. S12†). This is an improvement over previous studies, where purities >95% were reported.[24] Based on TLC and HPLC analysis, the remaining impurity was mainly caused by residual nucleoside/nucleo-

 This journal is © The Royal Society of Chemistry 2024

Open Access Article. Published on 14 octobre 2024. Downloaded on 25/01/2026 09:27:58.
This article is licensed under a Creative Commons Attribution 3.0 Unported Licence.

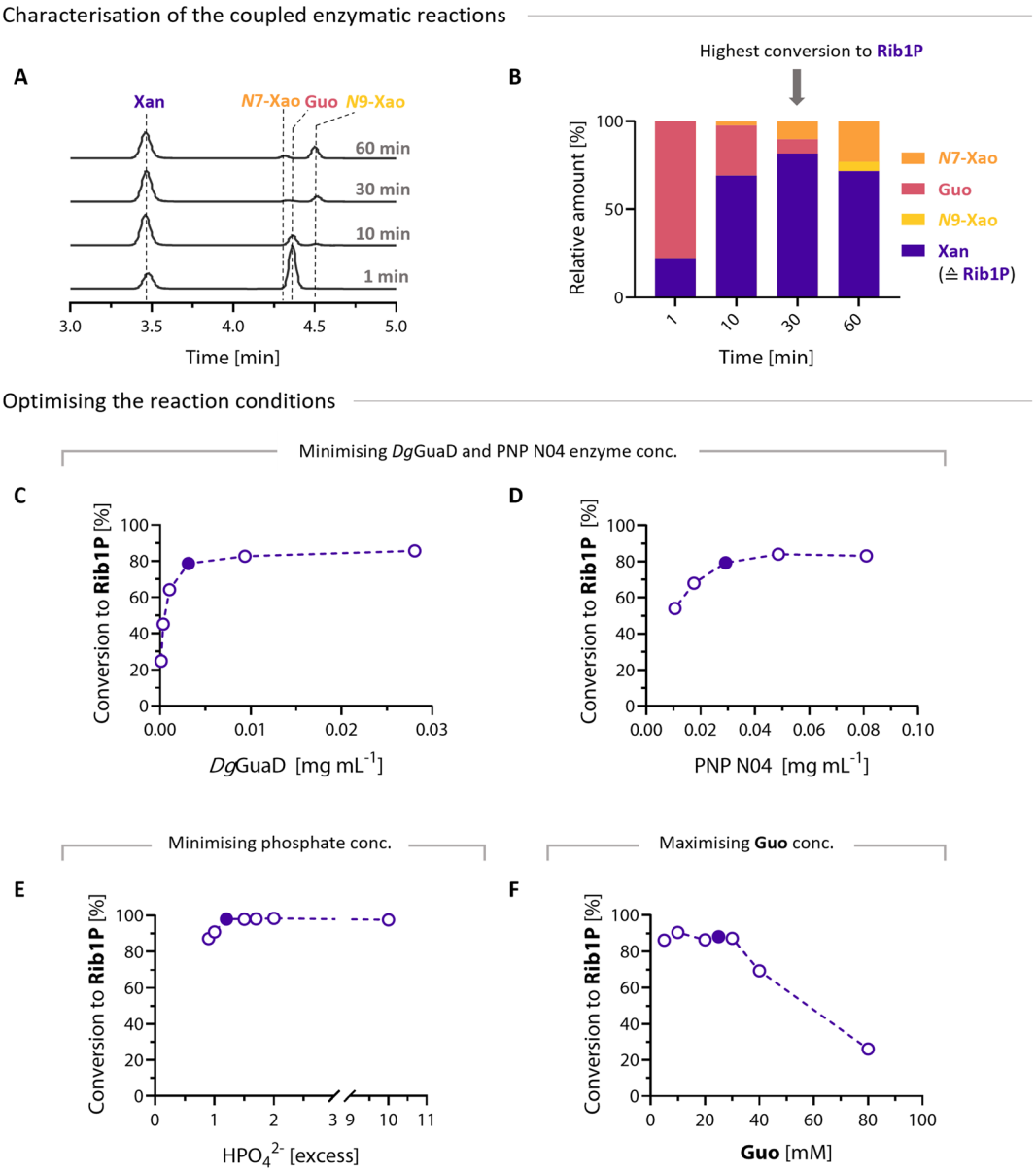

Fig. 2 GuaD coupled synthesis of **Rib1P**. (A) Representative HPLC chromatograms (recorded at λ = 260 nm) show the time course of the PNP N04 and *Dg*GuaD biocatalytic cascade. Please note the different extinction coefficients of the nucleosides and nucleobases (Fig. S11†). (B) Time course of the conversion of **Guo** to **Xan** and the byproducts ***N*9-Xao** and ***N*7-Xao**. (C–F) Optimisation of the PNP/GuaD cascade by varying *Dg*GuaD concentrations (C), PNP N04 concentrations (D), phosphate concentrations (E) and **Guo** concentration (F). Full-marked points represent the best conditions used for further experiments.

base. Other impurities that are not UV-active, however, remained unknown.

To validate the compatibility of the **Rib1P** with enzymatic glycosylation reactions, we used the material of the second batch in combination with different halogenated uridine bases (**5-F-Ura**, **5-Br-Ura**, **5-I-Ura**). In the reaction, equilibrium conversions were between 65 and 75% with an equimolar concentration of **Rib1P** compared to the halogenated nucleobases and matched well with calculated conversions based on the available equilibrium constants (Fig. 3C).[16] This demonstrates that impurities in the **Rib1P** preparations do not affect the usefulness of the material in glycosylation reactions. Hence, our **Rib1P** can be envisioned as being applied to difficult-to-access products, as recently shown for 5-ethynyluridine.[17]

Environmental impact of Rib1P synthesis routes

To estimate the environmental burden of (chemo)enzymatic **Rib1P** synthesis routes, we compared our cascade approach with other published methods that are (i) NP-based, (ii) use available substrates and enzymes, and (iii) give straightforward access to crystalline **Rib1P**-salts. Hence, the methods described by Kamel *et al.*[24] and Fateev *et al.*[23] (enzymatic approach start-

Open Access Article. Published on 14 octobre 2024. Downloaded on 25/01/2026 09:27:58.
This article is licensed under a Creative Commons Attribution 3.0 Unported Licence.

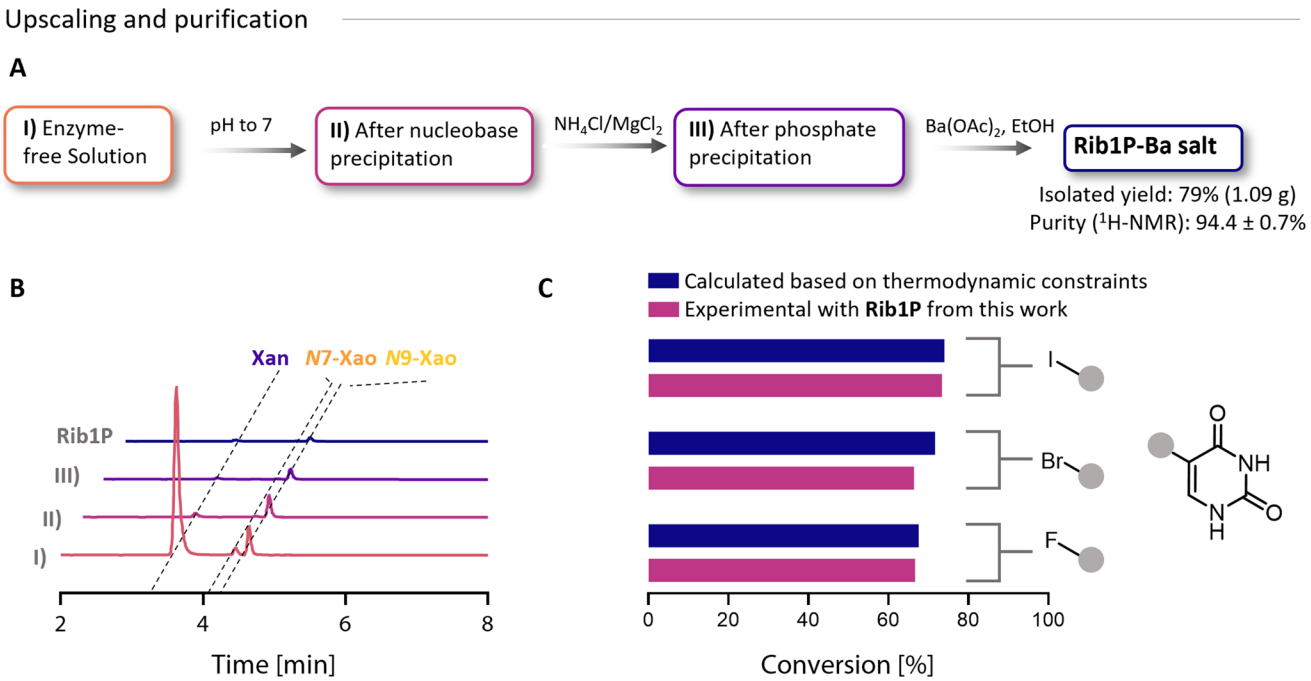

Fig. 3 Purification and gram-scale synthesis of **Rib1P**. (A) Purification process. Yield and purity are exemplary, as shown for the **Rib1P** synthesis of batch 2. Purity was determined by ^{1}H-NMR. (B) Corresponding HPLC chromatograms for the purification steps (recorded at λ = 260 nm). Please note the different extinction coefficients of the nucleosides and -bases (Fig. S11†). (C) Experimental validation of **Rib1P** purity *via* direct glycosylation of halogenated pyrimidines. The calculated values were taken from the ref. 16.

ing from uridine) and by Varizhuk *et al.*[29] (chemoenzymatic method starting from **7-Me-Guo**) were selected. Both the CHEM21 Zero Pass tool[46] and *E*-factor calculations[47–49] were applied. CHEM21 Zero Pass allows for a simple evaluation of reactions with a flag system and can thereby evaluate reactions in early development. To different categories, the following flags are assigned: (i) green flag (good to go, >89%), (ii) amber flag (acceptable, some issues, 70–89%), and (iii) red flag (indicate the discontinuation of the method, <70%). To make the table more accessible for people with colour deficiencies,[50] the colours were changed from green, yellow, and red to yellow, orange, and red, respectively. However, as the stoichiometry, yield, and solvent do not impact the atom economy (AE) included in the CHEM21 Zero Pass tool, we were further interested in comparing the different methods by the *E*-factor. Here, the amount of waste is calculated per weight unit of product produced (simple *E*-factor, sEF), which can be expanded by considering solvents and water consumption (complete *E*-factor, cEF).

When analysing the three published methods with the CHEM21 tool, they created a red flag because of either low yields (Kamel *et al.* and Fateev *et al.*) or the need for toxic chemicals (Varizhuk *et al.*) (Table 1).[51] Indeed, dichloromethane, dimethylformamide, and diethyl ether are listed as highly avoidable solvents, and iodomethane causes severe environmental concerns (H410). In contrast, the biocatalytic cascade reported herein did not generate red flags for any categories.

E-Factor calculations for all four methods (detailed information is provided in the ESI†) demonstrated that our cascade approach showed the lowest sEF (0.9 *vs.* 3.7, 8.9 and 5.1). In contrast, the cEF of our method was by factors of ~3.0 and ~1.5 higher compared to the methods described by Kamel

Table 1 Evaluation of the biocatalytic cascade for synthesising ribose-1-phosphate

	CHEM21 tool						Waste production	
	Yield [%]	Conv. [%]	*S* [%]	AE [%]	Solvents	Health & safety	sEF	cEF
Fateev *et al.*[23]	31	34	92	77	No flag	No flag	5.1	570
Kamel *et al.*[24]	25	40	63	77	No flag	No flag	8.9	285
Varizhuk *et al.*[29]	79	99	80	56	Et_2O, DMF, DCM	DMF, MeI	3.7	2816
This work	79	88	90	71	No flag	No flag	0.9	847

Conv. = conversion, S = selectivity, AE = atom economy, EtOH = ethanol, DMF = *N*,*N*-dimethylformamide, DCM = dichloromethane, Et_2O = diethyl ether, MeI = iodomethane. sEF = simple *E*-factor, cEF = complete *E*-factor. The colours of the CHEM21 tool were changed for accessibility.

This journal is © The Royal Society of Chemistry 2024

Open Access Article. Published on 14 octobre 2024. Downloaded on 25/01/2026 09:27:58. This article is licensed under a Creative Commons Attribution 3.0 Unported Licence.

et al. and Fateev *et al.* (Table 1). However, a ~3.3-fold reduction in the cEF was obtained compared to the other high-yielding chemoenzymatic approach described by Varizhuk *et al.* Solvents for purification and isolation of **Rib1P** had by far the most significant impact on the cEF values, as is typical for workup procedures.[52] Therefore, future studies should focus on reducing the use of solvents (including water), *e.g.*, by optimising the downstream processing or achieving even higher substrate loadings (*e.g.*, by running slurry-to-slurry reactions).

Conclusion

In conclusion, we present an improved biocatalytic process for the one-pot synthesis of **Rib1P**. By coupling a selective guanine deaminase to the NP-catalysed **Guo** cleavage, **Gua** was efficiently deaminated to **Xan**, hence shifting the reaction towards almost complete **Guo** cleavage. We demonstrate that this biocatalytic approach decreases the need for toxic reagents and purification steps, reducing the overall environmental burden of **Rib1P** synthesis. Due to the wide substrate spectrum of NPs, our approach offers the opportunity to produce a wide range of P1Ps. We expect our work to facilitate biocatalytic access to many sought-after nucleoside analogues by providing straightforward access to P1Ps as springboard synthons.

Accessibility statement

The data presented in this manuscript are depicted using scientific colour maps. Since *ca.* 4% of the human population is colour vision-deficient, we made a conscious effort to avoid unscientific uses of colour, such as colour ambiguities and other biases that could lead to misrepresentation, limited accessibility, or loss of information upon reduction of the colour space.[50] Thus, all figures herein were created using the scientific colour map *plasma* or *viridis*, which retains colour-coded information for all readers.

Author contributions

Conceptualisation: JM, SW, FK, and AK; data curation: JM; formal analysis: JM, LN, and AD; funding acquisition: PN and AK; investigation: JM, JB, CB, AD, LN, and SK; methodology: JM, SW, AK; project administration: PN and AK; resources: PN and AK; software, supervision: SW, FK, PN and AK; validation, visualisation: JM; writing – original draft: JM; writing – review & editing: all authors.

Data availability

The supplementary material and experiments are in the ESI.† Additionally, all raw MS and NMR data, as well as each figure's source data (when applicable) from the main manuscript and ESI,† are freely available externally at zenodo.org (ref. 53).

Conflicts of interest

AK is the CEO of the biotech company BioNukleo GmbH. SW was a scientist at BioNukleo GmbH, and PN is an advisory board member. At the time of the conceptualisation of this work, FK was a scientist at BioNukleo GmbH. The remaining authors declare no conflicts of interest.

Acknowledgements

This work was supported by Einstein Center of Catalysis/Berlin International Graduate School of Natural Sciences and Engineering (EC^2/BIG-NSE) as JM obtained an EC^2/BIG-NSE PhD scholarship. The authors thank Samantha Voges (TU Berlin, NMR Department) for assistance with NMR analyses. We additionally thank the Center for Mass Spectrometry at TU Berlin for HRMS analyses. Furthermore, we thank Sarah Kamel for providing information on her synthesis protocols.

References

1 C. S. Alexeev, M. S. Drenichev, E. O. Dorinova, R. S. Esipov, I. V. Kulikova and S. N. Mikhailov, Use of Nucleoside Phosphorylases for the Preparation of 5-Modified Pyrimidine Ribonucleosides, *Biochim. Biophys. Acta, Proteins Proteomics*, 2020, **1868**(1), 140292, DOI: 10.1016/j.bbapap.2019.140292.

2 G. Liu, T. Cheng, J. Chu, S. Li and B. He, Efficient Synthesis of Purine Nucleoside Analogs by a New Trimeric Purine Nucleoside Phosphorylase from Aneurinibacillus Migulanus AM007, *Molecules*, 2020, **25**(1), 100, DOI: 10.3390/molecules25010100.

3 H. Yehia, S. Kamel, K. Paulick, P. Neubauer and A. Wagner, Substrate Spectra of Nucleoside Phosphorylases and Their Potential in the Production of Pharmaceutically Active Compounds, *Curr. Pharm. Des.*, 2017, **23**(45), 6913–6935, DOI: 10.2174/1381612823666171024155811.

4 H. Yehia, S. Westarp, V. Röhrs, F. Kaspar, R. T. Giessmann, H. F. T. Klare, K. Paulick, P. Neubauer, J. Kurreck and A. Wagner, Efficient Biocatalytic Synthesis of Dihalogenated Purine Nucleoside Analogues Applying Thermodynamic Calculations, *Molecules*, 2020, **25**(4), 934, DOI: 10.3390/molecules25040934.

5 A. O. Denisova, Y. A. Tokunova, I. V. Fateev, A. A. Breslav, V. N. Leonov, E. V. Dorofeeva, O. I. Lutonina, I. S. Muzyka, R. S. Esipov, A. L. Kayushin, I. D. Konstantinova, A. I. Miroshnikov, V. A. Stepchenko and I. A. Mikhailopulo, The Chemoenzymatic Synthesis of 2-Chloro- and 2-Fluorocordycepins, *Synthesis*, 2017, **49**(21), 4853–4860, DOI: 10.1055/s-0036-1590804.

6 T. A. Krenitsky, G. W. Koszalka and J. V. Tuttle, Purine Nucleoside Synthesis: An Efficient Method Employing Nucleoside Phosphorylases, *Biochemistry*, 1981, **20**(12), 3615–3621, DOI: 10.1021/bi00515a048.

Open Access Article. Published on 14 octobre 2024. Downloaded on 25/01/2026 09:27:58.
This article is licensed under a Creative Commons Attribution 3.0 Unported Licence.

7 S. Westarp, C. Benckendorff, J. Motter, V. Rohrs, Y. Sanghvi, P. Neubauer, J. Kurreck, A. Kurreck and G. J. Miller, Biocatalytic Nucleobase Diversification of 4′-Thionucleosides and Application of Derived 5-Ethynyl-4′-Thiouridine for RNA Synthesis Detection, *Angew. Chem., Int. Ed.*, 2024, **63**(33), e202405040, DOI: **10.1002/anie.202405040**.

8 V. E. Kataev and B. F. Garifullin, Antiviral Nucleoside Analogs, *Chem. Heterocycl. Compd.*, 2021, **57**(4), 326–341, DOI: **10.1007/s10593-021-02912-8**.

9 K. L. Seley-Radtke and M. K. Yates, The Evolution of Nucleoside Analogue Antivirals: A Review for Chemists and Non-Chemists. Part 1: Early Structural Modifications to the Nucleoside Scaffold, *Antiviral Res.*, 2018, **154**, 66–86, DOI: **10.1016/j.antiviral.2018.04.004**.

10 M. Guinan, C. Benckendorff, M. Smith and G. J. Miller, Recent Advances in the Chemical Synthesis and Evaluation of Anticancer Nucleoside Analogues, *Molecules*, 2020, **25**(9), 2050, DOI: **10.3390/molecules25092050**.

11 C. M. Galmarini, J. R. Mackey and C. Dumontet, Nucleoside Analogues and Nucleobases in Cancer Treatment, *Lancet Oncol.*, 2002, **3**(7), 415–424, DOI: **10.1016/S1470-2045(02)00788-X**.

12 P. Morais, H. Adachi and Y.-T. Yu, The Critical Contribution of Pseudouridine to mRNA COVID-19 Vaccines, *Front. Cell Dev. Biol.*, 2021, **9**, 789427, DOI: **10.3389/fcell.2021.789427**.

13 N. Pardi, M. J. Hogan, F. W. Porter and D. Weissman, mRNA Vaccines—a New Era in Vaccinology, *Nat. Rev. Drug Discovery*, 2018, **17**(4), 261–279, DOI: **10.1038/nrd.2017.243**.

14 J. Motter, C. M. M. Benckendorff, S. Westarp, P. Sunde-Brown, P. Neubauer, A. Kurreck and G. J. Miller, Purine Nucleoside Antibiotics: Recent Synthetic Advances Harnessing Chemistry and Biology, *Nat. Prod. Rep.*, 2024, **41**, 863–970, DOI: **10.1039/D3NP00051F**.

15 J. M. Thomson and I. L. Lamont, Nucleoside Analogues as Antibacterial Agents, *Front. Microbiol.*, 2019, **10**, 952, DOI: **10.3389/fmicb.2019.00952**.

16 F. Kaspar, R. T. Giessmann, P. Neubauer, A. Wagner and M. Gimpel, Thermodynamic Reaction Control of Nucleoside Phosphorolysis, *Adv. Synth. Catal.*, 2020, **362**(4), 867–876, DOI: **10.1002/adsc.201901230**.

17 F. Kaspar, F. Brandt, S. Westarp, L. Eilert, S. Kemper, A. Kurreck, P. Neubauer, C. R. Jacob and A. Schallmey, Biased Borate Esterification during Nucleoside Phosphorylase-Catalyzed Reactions: Apparent Equilibrium Shifts and Kinetic Implications, *Angew. Chem., Int. Ed.*, 2023, **62**(20), e202218492, DOI: **10.1002/anie.202218492**.

18 F. Kaspar, R. T. Giessmann, K. F. Hellendahl, P. Neubauer, A. Wagner and M. Gimpel, General Principles for Yield Optimization of Nucleoside Phosphorylase-Catalyzed Transglycosylations, *ChemBioChem*, 2020, **21**(10), 1428–1432, DOI: **10.1002/cbic.201900740**.

19 K. F. Hellendahl, F. Kaspar, X. Zhou, Z. Yang, Z. Huang, P. Neubauer and A. Kurreck, Optimized Biocatalytic Synthesis of 2-Selenopyrimidine Nucleosides by Transglycosylation, *ChemBioChem*, 2021, **22**(11), 2002–2009, DOI: **10.1002/cbic.202100067**.

20 J. A. McIntosh, T. Benkovics, S. M. Silverman, M. A. Huffman, J. Kong, P. E. Maligres, T. Itoh, H. Yang, D. Verma, W. Pan, H.-I. Ho, J. Vroom, A. M. Knight, J. A. Hurtak, A. Klapars, A. Fryszkowska, W. J. Morris, N. A. Strotman, G. S. Murphy, K. M. Maloney and P. S. Fier, Engineered Ribosyl-1-Kinase Enables Concise Synthesis of Molnupiravir, an Antiviral for COVID-19, *ACS Cent. Sci.*, 2021, **7**(12), 1980–1985, DOI: **10.1021/acscentsci.1c00608**.

21 M. A. Huffman, A. Fryszkowska, O. Alvizo, M. Borra-Garske, K. R. Campos, K. A. Canada, P. N. Devine, D. Duan, J. H. Forstater, S. T. Grosser, H. M. Halsey, G. J. Hughes, J. Jo, L. A. Joyce, J. N. Kolev, J. Liang, K. M. Maloney, B. F. Mann, N. M. Marshall, M. McLaughlin, J. C. Moore, G. S. Murphy, C. C. Nawrat, J. Nazor, S. Novick, N. R. Patel, A. Rodriguez-Granillo, S. A. Robaire, E. C. Sherer, M. D. Truppo, A. M. Whittaker, D. Verma, L. Xiao, Y. Xu and H. Yang, Design of an in Vitro Biocatalytic Cascade for the Manufacture of Islatravir, *Science*, 2019, **366**(6470), 1255–1259, DOI: **10.1126/science.aay8484**.

22 G. Tener, R. Wright and H. Khorana, A Synthesis of Alpha-D-Ribofuranose-1-Phosphate, *J. Am. Chem. Soc.*, 1956, **78**(2), 506–507, DOI: **10.1021/ja01583a078**.

23 I. V. Fateev, M. I. Kharitonova, K. V. Antonov, I. D. Konstantinova, V. N. Stepanenko, R. S. Esipov, F. Seela, K. W. Temburnikar, K. L. Seley-Radtke, V. A. Stepchenko, Y. A. Sokolov, A. I. Miroshnikov and I. A. Mikhailopulo, Recognition of Artificial Nucleobases by E. Coli Purine Nucleoside Phosphorylase versus Its Ser90Ala Mutant in the Synthesis of Base-Modified Nucleosides, *Chem. – Eur. J.*, 2015, **21**(38), 13401–13419, DOI: **10.1002/chem.201501334**.

24 S. Kamel, M. Weiß, H. F. T. Klare, I. A. Mikhailopulo, P. Neubauer and A. Wagner, Chemo-Enzymatic Synthesis of α-d-Pentofuranose-1-Phosphates Using Thermostable Pyrimidine Nucleoside Phosphorylases, *Mol. Catal.*, 2018, **458**, 52–59, DOI: **10.1016/j.mcat.2018.07.028**.

25 H. M. Kalckar, The Enzymatic Synthesis of Purine Ribosides, *J. Biol. Chem.*, 1947, **167**(2), 477–486, DOI: **10.1016/S0021-9258(17)31000-1**.

26 J. N. Artsemyeva, E. A. Remeeva, T. N. Buravskaya, I. D. Konstantinova, R. S. Esipov, A. I. Miroshnikov, N. M. Litvinko and I. A. Mikhailopulo, Anion Exchange Resins in Phosphate Form as Versatile Carriers for the Reactions Catalyzed by Nucleoside Phosphorylases, *Beilstein J. Org. Chem.*, 2020, **16**(1), 2607–2622, DOI: **10.3762/bjoc.16.212**.

27 W. Zhang, T. Turney, I. Surjancev and A. S. Serianni, Enzymatic Synthesis of Ribo- and 2′-Deoxyribonucleosides from Glycofuranosyl Phosphates: An Approach to Facilitate Isotopic Labeling, *Carbohydr. Res.*, 2017, **449**, 125–133, DOI: **10.1016/j.carres.2017.07.006**.

28 I. V. Kulikova, M. S. Drenichev, P. N. Solyev, C. S. Alexeev and S. N. Mikhailov, Enzymatic Synthesis of 2-Deoxyribose 1-Phosphate and Ribose 1 Phosphate and Subsequent

 This journal is © The Royal Society of Chemistry 2024

Open Access Article. Published on 14 octobre 2024. Downloaded on 25/01/2026 09:27:58. This article is licensed under a Creative Commons Attribution 3.0 Unported Licence.

Preparation of Nucleosides, *Eur. J. Org. Chem.*, 2019, **2019**(41), 6999–7004, DOI: 10.1002/ejoc.201901454.

29 I. V. Varizhuk, V. E. Oslovsky, P. N. Solyev, M. S. Drenichev and S. N. Mikhailov, Synthesis of α-D-Ribose 1-Phosphate and 2-Deoxy-α-D-Ribose 1-Phosphate Via Enzymatic Phosphorolysis of 7-Methylguanosine and 7-Methyldeoxyguanosine, *Curr. Protoc.*, 2022, **2**(1), e347, DOI: 10.1002/cpz1.347.

30 S. Beyaztaş and O. Arslan, Purification of Xanthine Oxidase from Bovine Milk by Affinity Chromatography with a Novel Gel, *J. Enzyme Inhib. Med. Chem.*, 2015, **30**(3), 442–447, DOI: 10.3109/14756366.2014.943204.

31 C. Chen, G. Cheng, H. Hao, M. Dai, X. Wang, L. Huang, Z. Liu and Z. Yuan, Mechanism of Porcine Liver Xanthine Oxidoreductase Mediated N-Oxide Reduction of Cyadox as Revealed by Docking and Mutagenesis Studies, *PLoS One*, 2013, **8**(9), e73912, DOI: 10.1371/journal.pone.0073912.

32 M. R. Rashidi, M. H. Soruraddin, F. Taherzadeh and A. Jouyban, Catalytic Activity and Stability of Xanthine Oxidase in Aqueous-Organic Mixtures, *Biochemistry*, 2009, **74**(1), 97–101, DOI: 10.1134/S0006297909010155.

33 C.-H. Wang, T.-X. Zhao, M. Li, C. Zhang and X.-H. Xing, Characterization of a Novel Acinetobacter Baumannii Xanthine Dehydrogenase Expressed in Escherichia Coli, *Biotechnol. Lett.*, 2016, **38**(2), 337–344, DOI: 10.1007/s10529-015-1986-y.

34 M. Zarepour, K. Kaspari, S. Stagge, R. Rethmeier, R. R. Mendel and F. Bittner, Xanthine Dehydrogenase AtXDH1 from Arabidopsis Thaliana Is a Potent Producer of Superoxide Anions via Its NADH Oxidase Activity, *Plant Mol. Biol.*, 2010, **72**(3), 301–310, DOI: 10.1007/s11103-009-9570-2.

35 S. Leimkühler, R. Hodson, G. N. George and K. V. Rajagopalan, Recombinant Rhodobacter Capsulatus Xanthine Dehydrogenase, a Useful Model System for the Characterization of Protein Variants Leading to Xanthinuria I in Humans, *J. Biol. Chem.*, 2003, **278**(23), 20802–20811, DOI: 10.1074/jbc.M303091200.

36 A. Kunka, S. M. Marques, M. Havlasek, M. Vasina, N. Velatova, L. Cengelova, D. Kovar, J. Damborsky, M. Marek, D. Bednar and Z. Prokop, Advancing Enzyme's Stability and Catalytic Efficiency through Synergy of Force-Field Calculations, Evolutionary Analysis, and Machine Learning, *ACS Catal.*, 2023, **13**(19), 12506–12518, DOI: 10.1021/acscatal.3c02575.

37 F. Peccati, S. Alunno-Rufini and G. Jiménez-Osés, Accurate Prediction of Enzyme Thermostabilization with Rosetta Using AlphaFold Ensembles, *J. Chem. Inf. Model.*, 2023, **63**(3), 898–909, DOI: 10.1021/acs.jcim.2c01083.

38 H. Wu, Q. Chen, W. Zhang and W. Mu, Overview of Strategies for Developing High Thermostability Industrial Enzymes: Discovery, Mechanism, Modification and Challenges, *Crit. Rev. Food Sci. Nutr.*, 2023, **63**(14), 2057–2073, DOI: 10.1080/10408398.2021.1970508.

39 C. Vieille and G. J. Zeikus, Hyperthermophilic Enzymes: Sources, Uses, and Molecular Mechanisms for Thermostability, *Microbiol. Mol. Biol. Rev.*, 2001, **65**(1), 1–43, DOI: 10.1128/mmbr.65.1.1-43.2001.

40 B. L. Zamost, H. K. Nielsen and R. L. Starnes, Thermostable Enzymes for Industrial Applications, *J. Ind. Microbiol.*, 1991, **8**(2), 71–81, DOI: 10.1007/BF01578757.

41 N. K. Gupta and M. D. Glantz, Isolation and Characterization of Human Liver Guanine Deaminase, *Arch. Biochem. Biophys.*, 1985, **236**(1), 266–276, DOI: 10.1016/0003-9861(85)90626-5.

42 D. Mahor and G. S. Prasad, Biochemical Characterization of Kluyveromyces Lactis Adenine Deaminase and Guanine Deaminase and Their Potential Application in Lowering Purine Content in Beer, *Front. Bioeng. Biotechnol.*, 2018, **6**, 180, DOI: 10.3389/fbioe.2018.00180.

43 J. Kim, S. I. Park, C. Ahn, H. Kim and J. Yim, Guanine Deaminase Functions as Dihydropterin Deaminase in the Biosynthesis of Aurodrosopterin, a Minor Red Eye Pigment of Drosophila, *J. Biol. Chem.*, 2009, **284**(35), 23426–23435, DOI: 10.1074/jbc.M109.016493.

44 S. Westarp, F. Brandt, L. Neumair, C. Betz, A. Dagane, S. Kemper, C. R. Jacob, P. Neubauer, A. Kurreck and F. Kaspar, Nucleoside Phosphorylases Make N7-Xanthosine, *Nat. Commun.*, 2024, **15**(1), 3625, DOI: 10.1038/s41467-024-47287-4.

45 J. H. Lister and D. S. Caldbick, An Investigation into the Factors Governing the Aqueous Solubility of Xanthine (Purine-2,6-Dione), *J. Appl. Chem. Biotechnol.*, 1976, **26**(1), 351–354, DOI: 10.1002/jctb.5020260151.

46 C. R. McElroy, A. Constantinou, L. C. Jones, L. Summerton and J. H. Clark, Towards a Holistic Approach to Metrics for the 21st Century Pharmaceutical Industry, *Green Chem.*, 2015, **17**(5), 3111–3121, DOI: 10.1039/C5GC00340G.

47 F. Kaspar, M. R. L. Stone, P. Neubauer and A. Kurreck, Route Efficiency Assessment and Review of the Synthesis of β-Nucleosides via N-Glycosylation of Nucleobases, *Green Chem.*, 2021, **23**(1), 37–50, DOI: 10.1039/D0GC02665D.

48 R. A. Sheldon, The E Factor: Fifteen Years On, *Green Chem.*, 2007, **9**(12), 1273–1283, DOI: 10.1039/B713736M.

49 R. A. Sheldon, The E Factor 25 Years on: The Rise of Green Chemistry and Sustainability, *Green Chem.*, 2017, **19**(1), 18–43, DOI: 10.1039/C6GC02157C.

50 F. Kaspar and F. Crameri, Coloring Chemistry—How Mindful Color Choices Improve Chemical Communication, *Angew. Chem., Int. Ed.*, 2022, **61**(16), e202114910, DOI: 10.1002/anie.202114910.

51 D. Prat, A. Wells, J. Hayler, H. Sneddon, C. R. McElroy, S. Abou-Shehada and P. J. Dunn, CHEM21 Selection Guide of Classical- and Less Classical-Solvents, *Green Chem.*, 2015, **18**(1), 288–296, DOI: 10.1039/C5GC01008J.

52 F. Kaspar, M. R. L. Stone, P. Neubauer and A. Kurreck, Route Efficiency Assessment and Review of the Synthesis of β-Nucleosides via N-Glycosylation of Nucleobases, *Green Chem.*, 2021, **23**(1), 37–50, DOI: 10.1039/D0GC02665D.

53 J. Motter, Data for "A Deamination-Driven Biocatalytic Cascade for the Synthesis of Ribose-1-Phosphate", *Zenodo*, 2024, DOI: 10.5281/zenodo.10604602.